Electronic Supplementary Material (ESI) for Journal of Materials Chemistry A.

Supporting Information

Carbon and Binder-Free 3D Porous Perovskite Oxide Air Electrode for Rechargeable Lithium-oxygen Batteries

Thien Viet Pham, Hai Peng Guo, Wen Bin Luo, Shu Lei Chou, Jia Zhao Wang*, and Hua Kun Liu*

Experimental section

Synthesis of $LaNiO_3$, $LaNi_{0.9}Cu_{0.1}O_3$, and $LaNi_{0.9}Co_{0.1}O_3$ on Ni foam: $LaNiO_3$ on Ni foam was synthesized by a hydrothermal process. 1 mmol $La(NO_3)_3 \cdot 6H_2O$, 1 mmol $Ni(NO_3)_2 \cdot 6H_2O$, and 14 mmol KOH were dissolved in 45 mL of water. Nickel foam was cut into circular shapes 1.9 cm in diameter. Then, it was immersed in 6 M HCl solution to remove any oxide surface layers. Afterwards, the nickel foam and the aqueous solution were transferred to a Teflon-lined stainless-steel autoclave, which was sealed and maintained at 160 ^oC for 8 h. Finally, the product was taken out, washed, vacuum dried and then thermally treated at 400 ^oC in nitrogen for 2 h. The mass loading of $LaNiO_3$ on Ni foam was calculated from the difference in weight between the pristine Ni foam and the $LaNiO_3$ coated foam. The same hydrothermal process with different amounts of precursors was carried out to dope $LaNiO_3$ with Cu and Co. The quantity of 0.1 mmol of $Cu(NO_3)_2 \cdot 3H_2O$ or 0.1 mmol of $Co(NO_3)_2 \cdot 6H_2O$ was added to the aqueous solution to synthesize $LaNi_{0.9}Cu_{0.1}O_3$ and $LaNi_{0.9}Co_{0.1}O_3$ on Ni foam.

Characterization: All the samples were characterized by X-ray powder diffraction (XRD; GBC MMA) with Cu Kα radiation that was operated over a 2θ range of 15°–80°. The morphological studies were performed by field emission scanning electron microscopy (FE-SEM; JEOL-JSM-7500). Scanning transmission electron microscopy (STEM; JEOL ARM-200F), selected area electron diffraction (SAED), and TEM energy-dispersive X-ray spectroscopy (EDS) were used to investigate the single nanosheet structure and the doping effects of Cu and Co on $LaNiO_3$. Prior to the XRD analysis of the fully discharged cathode, the cell was opened in a glove box. The discharged sample was sealed with Kapton tape when transferred from the glove box to the atmosphere to avoid any reaction of the final products with moisture.

Electrochemical measurements: All the cells were assembled in an argon-filled glove box, using the catalyst on Ni foam as cathode, a glass fibre separator, a lithium metal foil anode, and an electrolyte containing 1 M $LiCF_3SO_3$ in TEGDME. For the TTF experiment, 0.1 mM TTF was added to the electrolyte as redox mediator. For CV testing, the cells were sealed in a self-designed bottle in the glove box. Then, the bottle was transferred to the atmosphere, unsealed, filled with O_2, and sealed again for CV testing. The CVs were obtained between 2 V and 4.5 V at a scan rate of 0.2 mV s^{-1}. In these tests, $LaNi_{0.9}Cu_{0.1}O_3$ or $LaNi_{0.9}Co_{0.1}O_3$ on Ni foam acted as the working electrode. On the other hand, lithium foil served as both counter and reference electrode. All battery tests were carried out on LAND CT 2001A multi-channel battery testers at room temperature in oxygen atmosphere. The discharge-charge cycling was performed with the specific capacity limited to 1000 mAh g^{-1} at a current density of 0.1 mA cm^{-2}. All the potentials throughout this paper are referred to the potential of the Li/Li^+ standard couple.

The aqueous electrochemical tests involving a rotating disk electrode (RDE) were carried out using a computer-controlled potentiostat (Biological VMP3) with a typical three-electrode cell, including a platinum wire as the counter electrode and an Ag/AgCl (saturated KCl filled) electrode as the reference electrode. The working electrodes were glassy carbon (GC) disk electrodes (5 mm in diameter) loaded with the respective active material inks. Typically, 5 mg of sample and 100 μL of 5 wt% Nafion® solution were dispersed in 1 mL water/isopropanol (3/1; v/v) solution and ultrasonicated for 30 min to form a uniform catalyst ink (~ 5 mg ml^{-1}). A total of 4.5 μL of the well-dispersed catalyst ink was applied on a pre-polished GC disk electrode. The as-prepared electrodes were dried at room temperature overnight prior to the electrochemical tests. The detailed kinetic analysis was conducted according to Koutecky-Levich plots $\frac{1}{j}=\frac{1}{j^{k}}+\frac{1}{Bw^{0.5}}$

(1)

where j is the current density, j_k is the kinetic current, and B is the Levich slope, which is given by

$$B = 0.2nF(D_{O_2})^{2/3}\nu^{-1/6}C_{O_2} \qquad (2)$$

Here, n is the number of electrons transferred in the reduction of one O_2 molecule, F is the Faraday constant (F = 96 485 C mol^{-1}), D_{O_2} is the diffusion coefficient of O_2 (D_{O_2} = 1.9 × 10^{-5} cm^2 s^{-1}), ν is the kinematic viscosity for KOH (ν = 0.01 cm^2 s^{-1}), and C_{O_2} is the concentration of O_2 in the solution (C_{O_2} = 1.2 × 10^{-6} mol cm^{-3}). The constant 0.2 is adopted when the rotation speed is expressed in rpm. According to Equations (1) and (2), the number of electrons transferred *(n)* can be obtained from the slope of the Koutecky–Levich plot of j^{-1} versus $\omega^{-1/2}$.

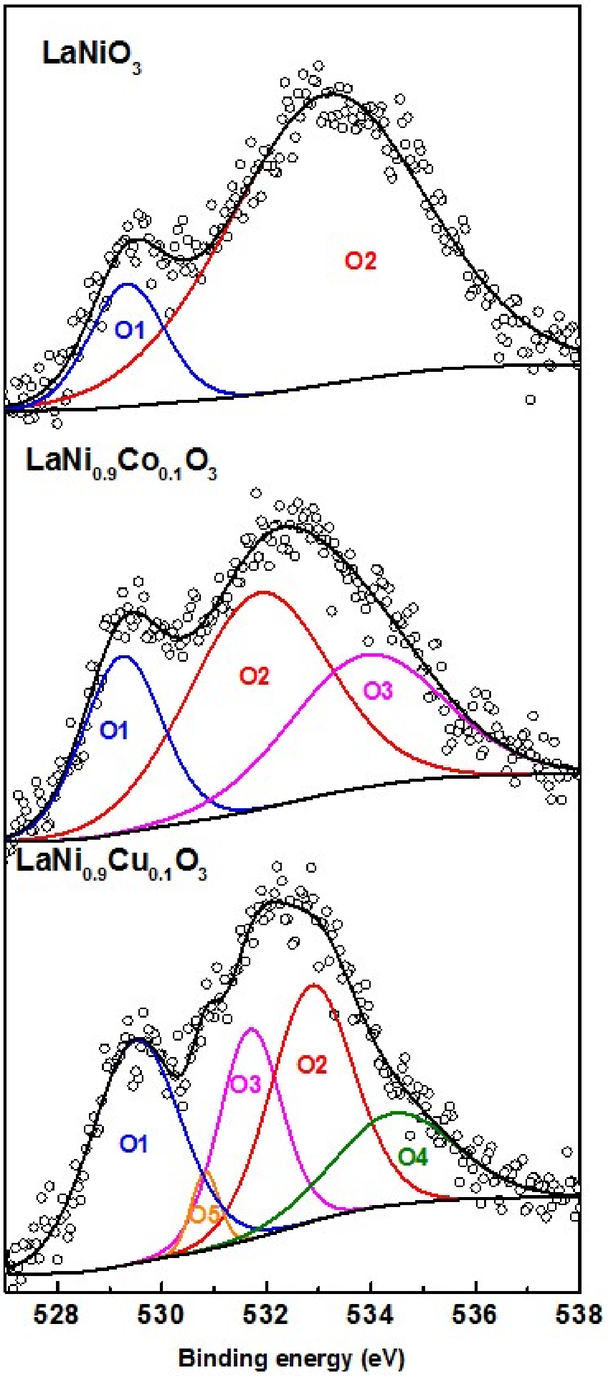

Figure S1. Oxygen spectra of LaNiO$_3$, LaNi$_{0.9}$Co$_{0.1}$O$_3$, LaNi$_{0.9}$Cu$_{0.1}$O$_3$ perovskite oxides.

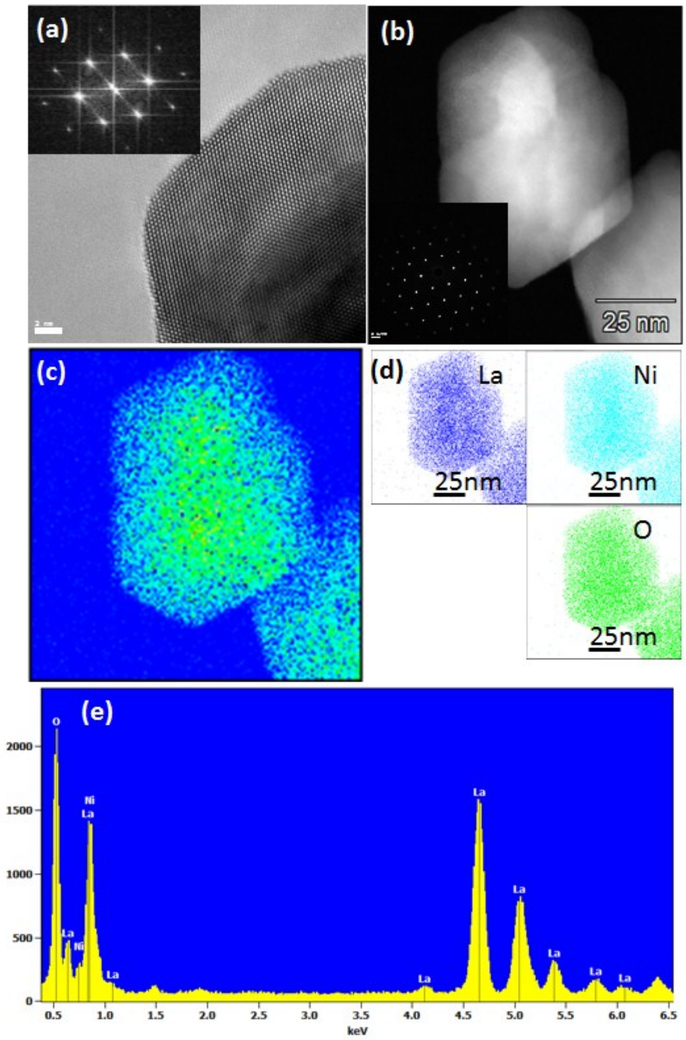

Figure S2. (a, b) TEM images of $LaNiO_3$ sample at different magnifications with insets containing the corresponding SAED patterns; (c) TEM EDS mapping of La, Ni, and O for a single $LaNiO_3$ nanosheet; (d) individual TEM EDS maps of La, Ni, and O elements for the same nanosheet; (e) EDS spectrum of $LaNiO_3$ sample.

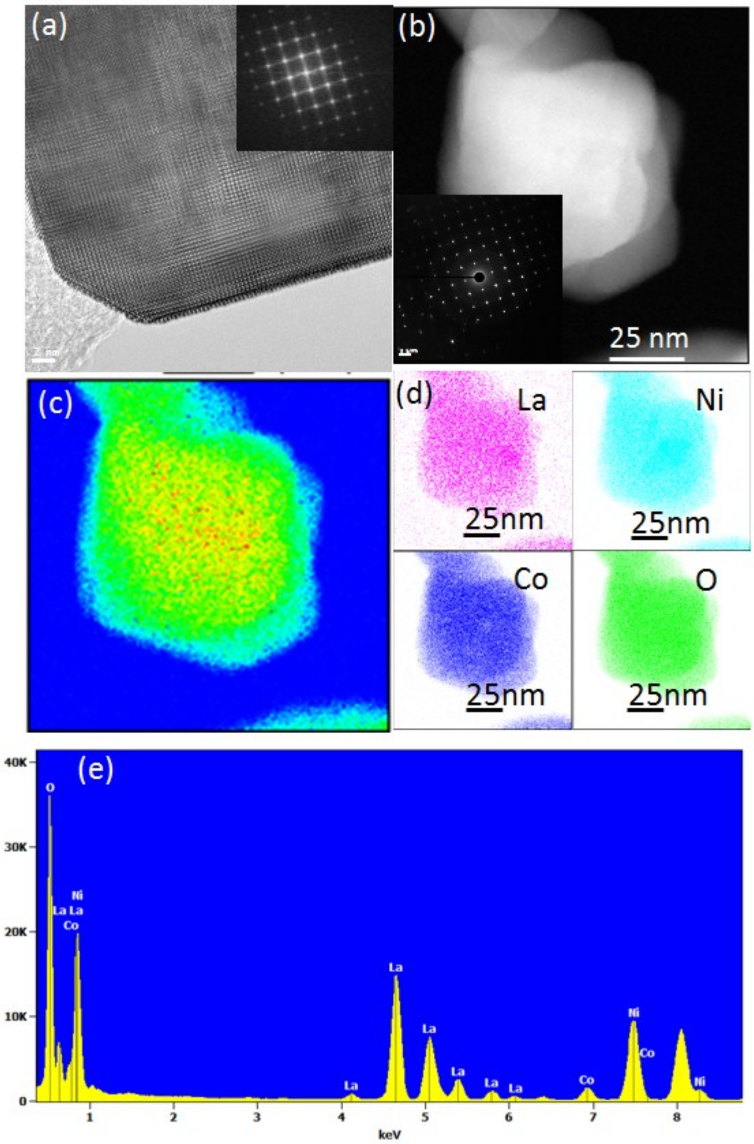

Figure S3. (a, b) TEM images of $LaNi_{0.9}Co_{0.1}O_3$ sample at different magnifications with the insets containing the corresponding SAED patterns; (c) TEM EDS mapping of La, Ni, Co, and O for a single $LaNi_{0.9}Co_{0.1}O_3$ nanosheet; (d) individual TEM EDS maps of La, Ni, Co, and O elements for the same nanosheet; (e) EDS spectrum of $LaNi_{0.9}Co_{0.1}O_3$ sample.

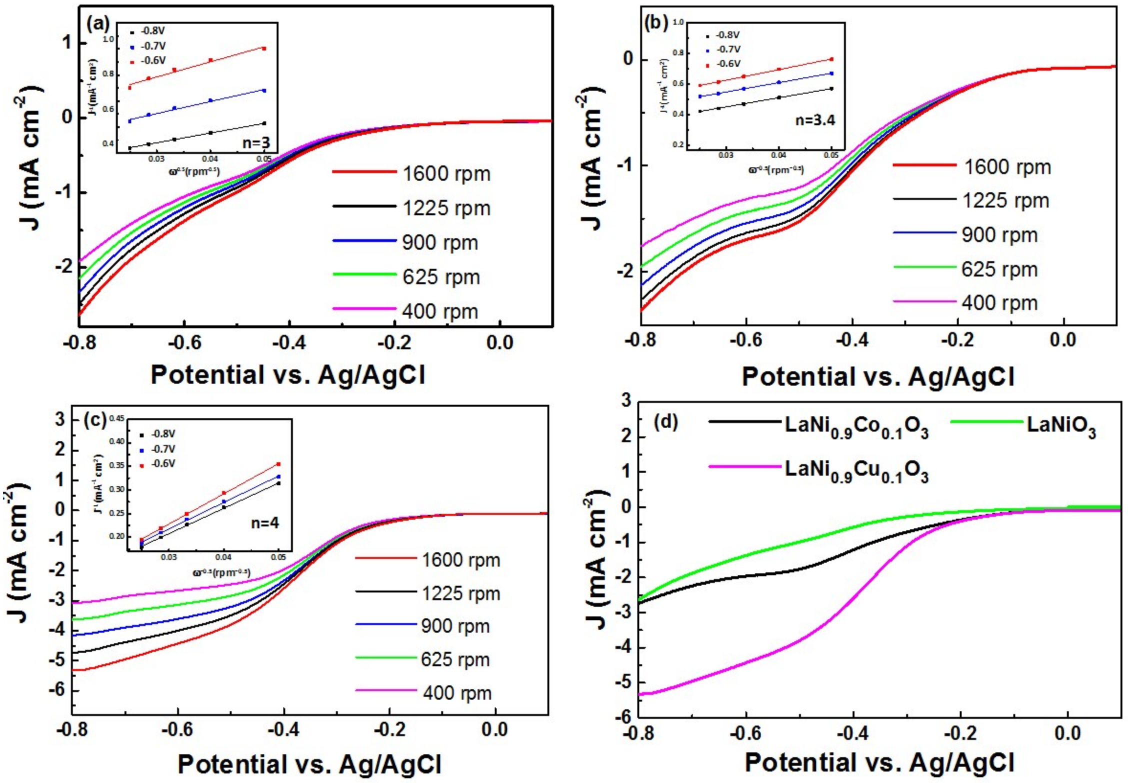

Figure S4. RDE curves of (a) $LaNiO_3$, (b) $LaNi_{0.9}Co_{0.1}O_3$, and (c) $LaNi_{0.9}Cu_{0.1}O_3$ in O_2-saturated 0.1 M KOH solution with various rotation speeds and a sweep rate of 10 mV s^{-1}; with the insets showing the corresponding K–L plots (J^{-1} versus $\omega^{-1/2}$) at different potentials. (d) RDE curves of $LaNiO_3$, $LaNi_{0.9}Cu_{0.1}O_3$, and $LaNi_{0.9}Co_{0.1}O_3$ at rotation speed of 1600 rpm.

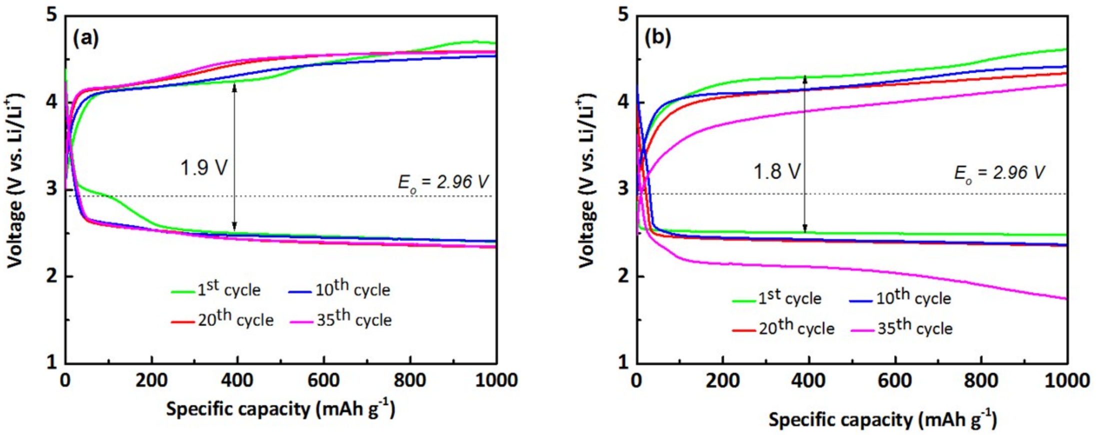

Figure S5 Cycling performance of (a) $LaNiO_3$ and (b) $LaNi_{0.9}Co_{0.1}O_3$ at 0. 1 mA cm^{-2} with capacity limited to 1000 mAh g^{-1}

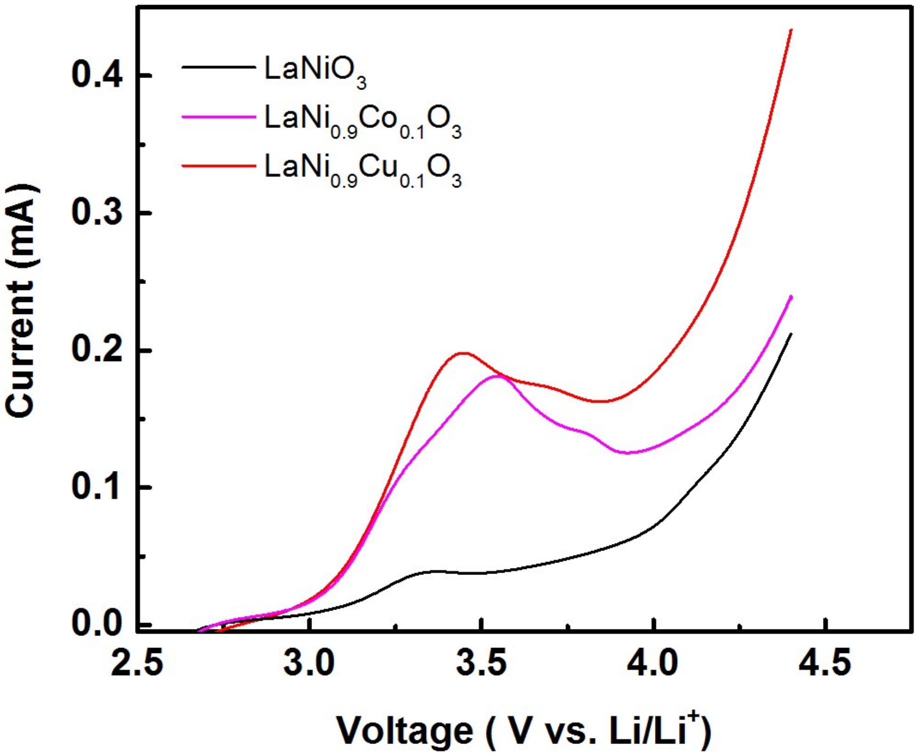

Figure S6. OER curves of (a) LaNiO$_3$, (b) LaNi$_{0.9}$Co$_{0.1}$O$_3$, and (c) LaNi$_{0.9}$Cu$_{0.1}$O$_3$ in O$_2$-saturated electrolyte at 0.2 mV s^{-1}.